Advances in Physics Theories and Applications
ISSN 2224-719X (Paper) ISSN 2225-0638 (Online)
Vol.49, 2015

Restriction of Particle Size and Lattice Strain through X-Ray Diffraction Peak Broadening Analysis of ZnO Nanoparticles

Khalid. Hellal. Harbbi Ahmed Alaa Ihsan
Department of Physics – College of Education (Ibn Al-Haitham) – University of Baghdad, Iraq.

Abstract
In this study have been determined the crystallite size and lattice strain of ZnO nanoparticles as shown in Figure (1) by using variance and integral breadth methods, and also used some other methods such as Scherrer and Williamson-Hall to calculate above parameters. In variance method we have calculated the values of crystallite size, mean square strain and lattice strain are (22.276 nm), (0.133473 x 10^{-3}) and (14.479 x 10^{-3}) respectively, and the crystallite size is (25.126 nm) as well as the lattice strain is (2.443 x 10^{-3}) by using integral breadth method. The other methods such as Scherrer which gives the value of crystallite size is (17.622 nm) and lattice strain is (6.036 x 10^{-3}), while the Williamson-Hall gives the following values: crystallite size is (22.063 nm) and the lattice strain is (1.192 x 10^{-3}).
Keywords: X-ray diffraction, Variance analysis method, integral breadth method.

1. Introduction

Diffraction lines of crystalline materials contain a wealth of microstructural information: The amount and distribution of the phases in the material, compositional inhomogeneity, the crystallite size and shape distributions, the crystallographic orientation distribution function. In many cases such information is not easily and statistically assured accessible by methods other than diffraction [1]. Microstructural parameters of a given material, crystallite size, distribution of sizes and crystallite strain, can be determined by X-ray diffraction methods, in combination with other techniques, especially electron microscopy and diffraction [2]. In 1912, the X-ray diffraction by crystals was discovered by Friedrich, Knipping and V. Laue [1]. X-ray diffraction is a convenient method for determining the mean size of nano crystallites in nano crystalline bulk materials. In 1918, the first scientist, Paul Scherrer, published his results in a paper that included what became known as the Scherrer equation. This can be attributed to the fact that "crystallite size" is not synonymous with "particle size", while X-ray diffraction is sensitive to the crystallite size inside the particles [3]. Laue in 1926 has considered the case of crystallites having the form of a parallelepiped and introduced the general form of the integral breadth, and also used Cauchy and Gaussian functions to model line profiles for the first time [4]. X-ray diffraction peak profile analysis is a powerful tool for the characterization of microstructures in crystalline materials. Diffraction peaks broaden when crystallites are small or the material contains lattice defects. The two effects can be separated on the basis of the different diffraction-order dependence of peak broadening. In 1953, the classical method have evolved during the past five decades: the Williamson-Hall (Williamson and Hall, 1953) procedure [5]. The method was first suggested by Tournarie (1956), and then developed by Wilson (1962a) [6]. Wilson in 1963 has applied the standard measures of position and dispersion used in statistical analysis (i.e. the centroid and variance) to powder diffraction, since the central moments of convoluted functions, can readily be separated. This approach has been reviewed recently by Berti (1993) [7].Klug and Alexander in 1974 have developed Scherrer, integral breadth and variance methods [7]. In this study to calculate the crystallite size and lattice strain XRD patterns of calcined samples of ZnO nanoparticles in the range of 2θ =30° to 70° were used as shown in Figure (1) [8].

2. Theory

2.1 The Variance method

The variance of the line profiles [W(2θ)] is defined as the second central moment of the distribution of diffracted intensities [I(2θ)] , and is therefore a measure of the line broadening. According to this definition, W(2θ) is calculated on the 2θ scale for a given truncation range (2θ) by the expression [9].

$$w(2\theta) = \frac{\int(2\theta - <2\theta>)^2 \,.\, I(2\theta)d(2\theta)}{\int I(2\theta)d(2\theta)} \quad \ldots\ldots\ldots\ldots (1)$$

With <2θ> being centroid of line profile [7].

$$< 2\theta > = \frac{\int 2\theta.\, I(2\theta)d(2\theta)}{\int I(2\theta)d(2\theta)} \quad \ldots\ldots\ldots\ldots (2)$$

May let range of Measurement $\sigma_1 + \sigma_2 = \sigma$ and express the linear of variance-range in for

$$w = w_0 + K\sigma \quad \ldots\ldots\ldots\ldots (3)$$

The variance coefficients (w_0 and K) of the line profiles can be evaluated empirically by a linear fit to the set of variance-range pairs determined directly by equation (1) [9].

The variance (W) of the X-ray line profile is given by

$$W = W_P + W_S + W_D \quad \ldots\ldots\ldots\ldots (4)$$

Where W_P, W_S, W_D is the factor corresponding to crystallite size, lattice strain, layer disorder respectively. The variance of the X-ray line profile is represented by [10].

$$W = \frac{\lambda \Delta 2\theta}{2\pi^2 P' cos\theta} + \frac{S\lambda^2}{cos^2\theta} \quad \text{.......... (5)}$$

S given by equation (6) [11-12].

$$S = \frac{<e^2> - B_D^2/\pi^2}{d^2} \quad \text{.......... (6)}$$

$$\frac{1}{P'} = \frac{1}{P} + \frac{B_D}{d} \quad \text{.......... (7)}$$

Where B_D is the integral width of the defect profile, $< e^2 >$ is the mean square strain, d is the inter planer spacing, $\Delta 2\theta$ = total angular range in 2θ scale over which the measurements are being made. P′ Is the apparent crystallite size from variance method; P is true crystallite size [10-11].

From Bragg's law [13].

$$4d^2 sin^2\theta = \lambda^2 \rightarrow d^2 = \lambda^2/4sin^2\theta \quad \text{.......... (8)}$$

$$2sin\theta = \lambda \rightarrow d = \frac{\lambda}{2sin\theta} \quad \text{.......... (9)}$$

Substitute equation (6) and (7) in (5) gives the following equation:

$$W = \frac{\lambda \Delta 2\theta}{2\pi^2 cos\theta}\left[\frac{1}{p} + \frac{B_D}{d}\right] + \frac{<e^2>\lambda^2}{d^2 cos^2\theta} - \frac{B_D{}^2}{\pi^2}\frac{\lambda^2}{d^2 cos^2\theta} \quad \text{.......... (10)}$$

Substitute equations (8) and (9) in (10) gives the following equation:

$$W = \frac{\lambda(\Delta 2\theta)}{2\pi^2 p cos\theta} + \frac{(\Delta 2\theta)B_D}{\pi^2}\frac{sin\theta}{cos\theta} - 4\frac{B_D{}^2}{\pi^2}\frac{sin^2\theta}{cos^2\theta} + 4 < e^2 > \frac{sin^2\theta}{cos^2\theta} \quad \text{.......... (11)}$$

Since $\frac{sin\theta}{cos\theta} = tan\theta$

$$W = \frac{\lambda(\Delta 2\theta)}{2\pi^2 p cos\theta} - \frac{B_D tan\theta}{\pi^2}[4 B_D tan\theta + (\Delta 2\theta)] + 4 < e^2 > tan^2\theta \quad \text{.......... (12)}$$

B_D Is commonly neglected in practical applications [7]. The numerical solution of size and strain parameter is conveniently carried out by neglecting B_D and arranging equation (12) and become to equation (13). It is assumed that the broadening of the x-ray line is due to the crystallite-size and strain only, the variance can be written as [14-15].

$$W_{2\theta} = \frac{\Delta 2\theta\lambda}{2\pi^2 P cos\theta} + 4tan^2\theta < e^2 > \quad \text{.......... (13)}$$

Multiplying equation (13) by $\frac{cos\theta}{\Delta 2\theta\lambda}$ we can get the following equation:

$$\frac{W_{2\theta}cos\theta}{\Delta 2\theta\lambda} = \frac{1}{2\pi^2 P} + \frac{4sin\theta tan\theta}{\Delta 2\theta\lambda} < e^2 > \quad \text{.......... (14)}$$

Also the relation between root mean square strain and lattice strain is [16].

$$< e^2 >^{1/2} = \sqrt{\frac{2}{\pi}}e \quad \text{.......... (15)}$$

The instrumental corrected broadening β_{hkl} [17] corresponding to the diffraction peaks was estimated using the equation

$$\beta_{hkl} = \sqrt{(\beta_{measured})^2 + (\beta_{instrumental})^2} \quad \text{.......... (16)}$$

2.2 Integral Breadth Method

The integral breadth (IB) method is frequently used in studies of the microstructure of materials for a quick estimation of the so-called 'size-strain' line broadening effect, mostly relating to the broadening caused by the average size of the crystallites (coherently scattering domains) and by lattice strains (often denoted as microstrains or lattice distortions) caused by, e.g. the presence of lattice defects [18].

$$\beta_i = A/I_0 \quad \text{.......... (17)}$$

A being the peak area and I_0 the height of observed line profile.In both the relation the peak broadening was attributed to effect of the diffracting coherent domain size. When the broadening is solely due to strain effect the following [19].

The peak broadening and its anisotropy were supposed to be caused by the dislocations in the crystals. According to Krivoglaz, the strain-induced part of the integral breadth β_i of a diffraction profile (expressed in S units, $s = 2sin\theta/\lambda$) related to the arrangement of the dislocations, with weak defect correlation, is given by [20].

$$(\beta_s)_i^D = 2es \quad \text{.......... (18)}$$

$$(\beta_s)_i^D = 4e\frac{sin\theta}{\lambda} \quad \text{.......... (19)}$$

Where $(\beta_{2\theta})_i^D = \frac{\lambda}{cos\theta}(\beta_s)_i^D$ integral breadth in the units of S [21]. .... (20)

Substitute equation (19) in (20) gives the following equations:

$$(\beta_{2\theta})_i^D = \frac{\lambda}{cos\theta}4e\frac{sin\theta}{\lambda} = 4e\frac{sin\theta}{cos\theta} \quad \text{.......... (21)}$$

$(\beta_{2\theta})_i^D = 4e\ tan\theta$ ……..…….. (22)

Scherrer for broadening resulting from small crystallite size alone [22].

$P = \frac{K\lambda}{\beta cos\theta} \rightarrow (\beta_{2\theta})_i^S = \frac{K\lambda}{Pcos\theta}$ ……..……..…….. (23)

In 2θ Scale, or

$(\beta_s)_i^S = \frac{cos\theta}{\lambda}\frac{K\lambda}{Dcos\theta} \rightarrow (\beta_s)_i^S = \frac{K}{D}$ ……..…….. (24)

On the S Scale

Wherein K of equation (24) has been set equal to unity [23, 24]. With regard due to effect of size (or due to stacking faults$(\beta_{2\theta})_i^S$) and widening induced by microstrain $(\beta_{2\theta})_i^D$, respectively [25].

According to Voigt method, the basic relationships between the integral breadths β_i are shown as the following equation: [21, 26].

$\beta_i = \beta_{Sc} + \beta_{Dc}$ (Cauchy/Cauchy) ……..…….. (25)

$\beta_i{}^2 = (\beta_{SG})^2 + (\beta_{DG})^2$ (Gaussian/ Gaussian) …….. (26)

Where β_{SC} and β_{DC} are the Cauchy components of size and strain integral breadth respectively and β_{SG} and β_{DG} are the corresponding Gaussian components [21].

Substitute equation (19) and (24) in (25) gives the following equation:

$(\beta_s)_i = \frac{1}{P} + 4e\ \frac{sin\theta}{\lambda}$ (Cauchy/Cauchy) …….. (27)

Substitute equation (19) and (24) in (26) gives the following equation:

$[(\beta_s)_i]^2 = \left[\frac{1}{P}\right]^2 + 16e^2\ \left[\frac{sin\theta}{\lambda}\right]^2$ (Gaussian/ Gaussian) …….. (28)

From equation (20) can obtain the following equation:

$(\beta_s)_i = \frac{(\beta_{2\theta})_i cos\theta}{\lambda}$ …….. (29)

Substitute equation (29) in (27) gives equation (30). The basic assumption of this method is that the both size and strain broadened profiles are of Cauchy (Lorentzian) shape. Based on this assumption, a mathematical relation was established between the integral breadth (β), volume weighted average crystallite size (P), and the lattice strain (e) as follows [24].

$\frac{(\beta_{2\theta})_i cos\theta}{\lambda} = \frac{1}{P} + 4e\ \frac{sin\theta}{\lambda}$ (Cauchy/Cauchy) …….. (30)

Substitute equation (29) in (28) gives equation (31). Gaussian squared method assuming a Gaussian–Gaussian profile, crystallite size and lattice strain parameters can be calculated [26].

$\left[\frac{(\beta_{2\theta})_i cos\theta}{\lambda}\right]^2 = \frac{1}{P^2} + 16e^2\ \left[\frac{sin\theta}{\lambda}\right]^2$ (Gaussian/ Gaussian) …….. (31)

According to Weidenthaler [28], the relationships between the integral breadth β and FWHM for Cauchy and for Gaussian profiles are described by the following equations [29-30]:

$\frac{\beta_{FWHM}}{\beta_i} = \frac{2}{\pi} = 0.6366$ For Cauchy profile …….. (32)

$\frac{\beta_{FWHM}}{\beta_i} = \sqrt{\frac{4ln2}{\pi}} = 0.9394$ For Gaussian profile …….. (33)

If $\frac{\beta_{FWHM}}{\beta_i}$ close to 0.6366, should use the integral breadth (Cauchy profile) equation (30) and if $\frac{\beta_{FWHM}}{\beta_i}$ close to 0.9394, should use the integral breadth (Gaussian profile) equation (31) to determine the crystallite size (P) and the lattice strain (e).

2.3 The Peak Position and the Peak Width (Broadening) Determination

There are two important measures in line profile analysis of power diffraction

- The peak position
- The peak width (broadening)

The peak position determined by Klug and Alexander in 1974 [7].

Full-Width at Half-Maximum intensity (FWHM): The overall width of line profile at half-maximum intensity measured above the background as shown in Figure (2).

$$FWHM = 2\theta_2 - 2\theta_1$$

2.4 Another analysis methods

2.4.1 Scherrer Method

XRD can be utilized to evaluate peak broadening with crystallite size and lattice strain due to dislocation [31]. The crystallite size determined by the X-ray line broadening method using the Scherer equation

$P = \left(\frac{K\lambda}{\beta_{hkl} cos\theta}\right)$ …….. (34)

Where P is the crystallite size in nanometers, where K=0.94, is the wavelength of the radiation (1.54056 Å for CuKα radiation), β_{hkl} is the full width at half maximum (FWHM) of the peak in radians, and θ is the Bragg angle [32].
Similarly, according to Wilson, the broadening due to lattice strain may be expressed by the relation:

$$\beta_s = \eta\, tan\theta \;\rightarrow\; e = \frac{\beta_s}{4tan\theta} \quad \ldots\ldots\ldots\ldots\ldots\ldots\ldots\ldots (35)$$

Where $(\beta_{hkl})_s$ is the peak broadening due to lattice strain η the strain distribution within the material, η = 4e and θ is the Bragg's angle [33].

2.4.2 Williamson-Hall Method

Crystal imperfections and distortion of strain-induced peak broadening are related by e ≈ βs/4tanθ. There is an extraordinary property of equation (34) which has the dependency on the diffraction angle θ. Scherrer-equation follows a 1/cosθ dependency but not tanθ as W-H method. This basic difference was that both microstructural causes small crystallite size and lattice strain occur together from the reflection broadening [34]. Depending on different θ positions the separation of size and strain broadening analysis is done using Williamson and Hall. The following results are the addition of the Scherrer equation and e ≈ βs/4tanθ [35].

$$\beta_{hkl} = \beta_S + \beta_D \quad \ldots\ldots\ldots\ldots\ldots\ldots\ldots\ldots (36)$$

$$\beta_{hkl} = \frac{K\lambda}{Pcos\theta} + 4e\, tan\theta \quad \ldots\ldots\ldots\ldots\ldots\ldots\ldots\ldots (37)$$

$$\beta_{hkl} = \frac{K\lambda}{Pcos\theta} + 4e\, \frac{sin\theta}{cos\theta}$$

According to the Williamson-Hall method [36], the individual contributions to the broadening of reflections can be expressed as

$$\beta_{hkl}cos\theta = \frac{K\lambda}{P} + 4esin\theta \quad \ldots\ldots\ldots\ldots\ldots\ldots\ldots\ldots (38)$$

Where *P* is the crystallite size and e is the lattice strain [37].

3. Results and Discussion

3.1 Variance analysis method

In this study we have analyzed line diffraction profile by variance method, from Figure (1) we have got 2θ and Intensity, ∑I/I$_{(peak)}$, ∑(2θ.I(2θ), then used equation (2) to obtain centroid (<2θ>), then got ∑(2θ-<2θ>)^2 .I(2θ) then used equation (1) to obtain variance $(W_{2\theta})$ for each peak of ZnO nanoparticles, the results are listed in Tables (1-2) as shown in Figures (3).

We calculated ∑I/I(peak), ∑(2θ.I(2θ), <2θ> and ∑(2θ-<2θ>)^2. I(2θ) of peak (100) as shown in Table 1. And the other peaks calculated by the same method.

We used our data from (Figure 1 and Table 2) to calculate $\frac{\boldsymbol{W(2\theta)Cos\theta}}{\boldsymbol{\lambda(\Delta 2\theta)}}$ and $\frac{\boldsymbol{4Sin\theta Tan\theta}}{\boldsymbol{\lambda(\Delta 2\theta)}}$, the results are listed in Table (3).

Where $W_{2\theta}$ is corrected by using equation (16), then transformed to radian. Δ2θ is set to the value of 2 and wavelength λ is 0.154056 nm

The expression $\frac{\boldsymbol{4Sin\theta Tan\theta}}{\boldsymbol{\lambda(\Delta 2\theta)}}$ is the x-axis and $\frac{\boldsymbol{W(2\theta)Cos\theta}}{\boldsymbol{\lambda(\Delta 2\theta)}}$ is the y-axis in variance plot as shown in Figure (4).

Figure 4 the variance plot used to calculate the crystallite size P and mean square strain $< e^2 >$ by equation (14). Graphically, the crystallite size P is obtained from the y-intercept and the strain is obtained from $< e^2 >$ which in turn is obtained from the slope.

$$< e^2 >= Slope\ ,\ P = \frac{1}{intercept*2\pi^2}$$

$$< e^2 > = 0.0001334733$$

We used equation (15) to calculate strain (*e*)

$$e = \sqrt{\frac{0.0001334733 * \pi}{2}} = 14.47961 * 10^{-3}$$

$$P = \frac{1}{0.00227412*2\pi^2} = 22.276973\ nm$$

3.2 Integral breadth analysis method

In this study we have analyzed line diffraction profile by integral breadth method, we have used Figure (1) to get 2θ and intensity, then used equation (17) to obtain integral breadth β_i for 20 steps to get $(\beta_i)_{Average}$ for each peak of ZnO nanoparticles, the results are listed in Tables (4) and as shown in Figure (5) .

We calculated $(\beta_i)_{Average}$ of peak (100) as shown in Table 3. And the other peaks calculated by the same method.

We have used equations (32-33) for each peak of ZnO nanoparticles to confirm if our peaks are Cauchy or Gaussian profiles, the the results are listed in Table (5).

In this study all peaks are following Gaussian profile as shown in Table (5).

In this study we used our data from (Figure 1 and Table 5) to calculate $\left(\frac{\beta_i cos\theta}{\lambda}\right)^2$ and $\left(\frac{sin\theta}{\lambda}\right)^2$, the results are listed in Table (6).
Where β_i is corrected by using equation (16), then transformed to radian. λ is set to the value of 0.154056 nm.
The expression $(sin\theta/\lambda)^2$ is the x-axis and $(\beta_i cos\theta/\lambda)^2$ is the y-axis in integral breadth plot as shown in Figure (6).
Figure 6 the Integral breadth plot have been used to calculate the crystallite size P and strain e by equation (31), since all the values of β_i follow Gaussian profile. Graphically, the crystallite size P is obtained from the y-intercept and the strain e is obtained from e^2 which in turn is obtained from the slope.

$16\,e^2 = Slope \;\;,\;\; P = \sqrt{\frac{1}{intercept}}$

$4e = \sqrt{Slope} \rightarrow e = \frac{\sqrt{Slope}}{4} = \frac{\sqrt{9.5563 * 10^{-5}}}{4}$

$e = 2.443 * 10^{-3}$

$P = \sqrt{\frac{1}{0.0015839568}}$

$P = 25.126\ nm$

3.3 Another analysis methods

3.3.1 Scherrer method

In this study we have used equations (34-35) to determine the crystallite size (P) and lattice strain (e) respectively, we have used Figure (1) to calculate FWHM as shown in Figure (2) and the results of crystallite size, lattice strain and FWHM are listed in Table (7).
The advantage of Scherrer method is the easiest method to apply it in order to calculate crystallite size and lattice strain.

3.3.2 Williamson-Hall method

In this study we have analyzed line diffraction profile by Williamson-Hall method, we have used Figure (1) to calculate FWHM (β_{hkl}) as shown in Figure (2) ,then we have used FWHM (β_{hkl}) and 2θ to determine the $\beta_{hkl}Cos\theta$ and $4Sin\theta$ for each peak of ZnO nanoparticles, the results are listed in Table (8).
The expression $4Sin\theta$ is the x-axis and $\beta_{hkl}Cos\theta$ is the y-axis in Williamson-Hall plot as shown in Figure (7).
Williamson-hall plot have been used to calculate the crystallite size P and the lattice strain (e) by using equation (38). Graphically, the crystallite size P is obtained from the y-intercept and the lattice strain e is obtained from the slope.

$e = Slope\ , P = \frac{K\lambda}{intercept}$

$e = 1.19225\ x\ 10^{-3}$

$P = \frac{0.94*0.154056}{0.0065636107}$

$P = 22.063\ nm$

3.4 Comparison among Variance, integral breadth, Scherrer and Williamson-Hall methods to determine crystallite size and lattice strain of ZnO nanoparticles

We have determined crystallite size and lattice strain of ZnO nanoparticles by using variance, integral breadth, Scherrer & Williamson-Hall X-ray diffraction line profile methods. The results are listed in Table (9).

Methods of Variance and Integral breadth give the most accurate results than Scherrer and Williamson-Hall methods due to these two methods of Variance and Integral breadth dependent on calculate the intensity by Segmenting diffraction line to many lines then collect these lines and make calculations of each method that procedure can reduce dramatically the proportion of error in the calculation intensity, while Scherrer and Williamson-Hall dependent on the full width at half maximum (FWHM) of the peak which it is Approximation method because of this method is relying on only two lines to calculate the intensity.

The results indicate that the variance is very sensitive to the range of integration $\Delta 2\theta = (2\theta_2 - 2\theta_1)$ The variance method give us higher Strain than integral breadth and Williamson-Hall methods due to the slope of the variance of the line profile as a function of the range of integration .

Variance method takes into account the total area of the peak (peak + Tails) due to tails of peak is increase the variance value ($W_{2\theta}$) thus increase the strain while integral breadth takes the area of peak and both Scherrer and Williamson-Hall take the full width at half maximum (FWHM) of the peak.

4. Conclusion

1. The main method it's variance in the chart of XRD. In this method can be get a good accurate results of crystallite size and lattice strain because removed all source of line broadening approximately, also this method

used total area under the curve of the peak.
2. The integral breadth determined the crystallite size and lattice strain after remove the instrumental broadening and used rectangular area of the peak. Therefore this method is accurate to analysis of the line profile XRD.
3. The Scherrer and Williamson-Hall methods give less accurate results of the crystallite size and lattice strain than variance and integral breadth methods. These methods are used the full width at half maximum (FWHM) of the peak which it is Approximation method.
4. All above methods give a good results to determine crystallite size and lattice strain but the variance method give the most accurate results because it is cover all the area of the peak and we know the value of high intensity give not accurate results to determine lattice parameters of structure lattice.

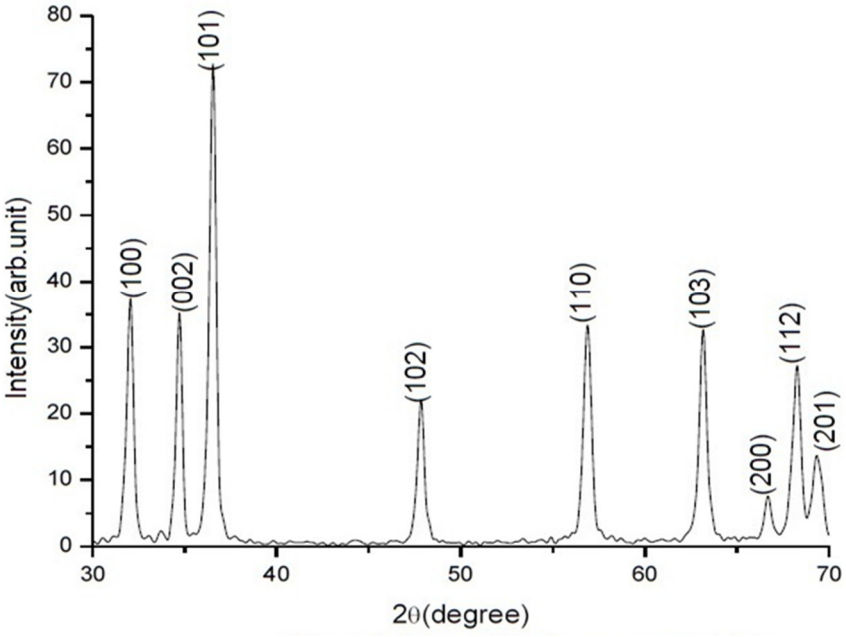

Figure 1: XRD of ZnO nanoparticles [8]

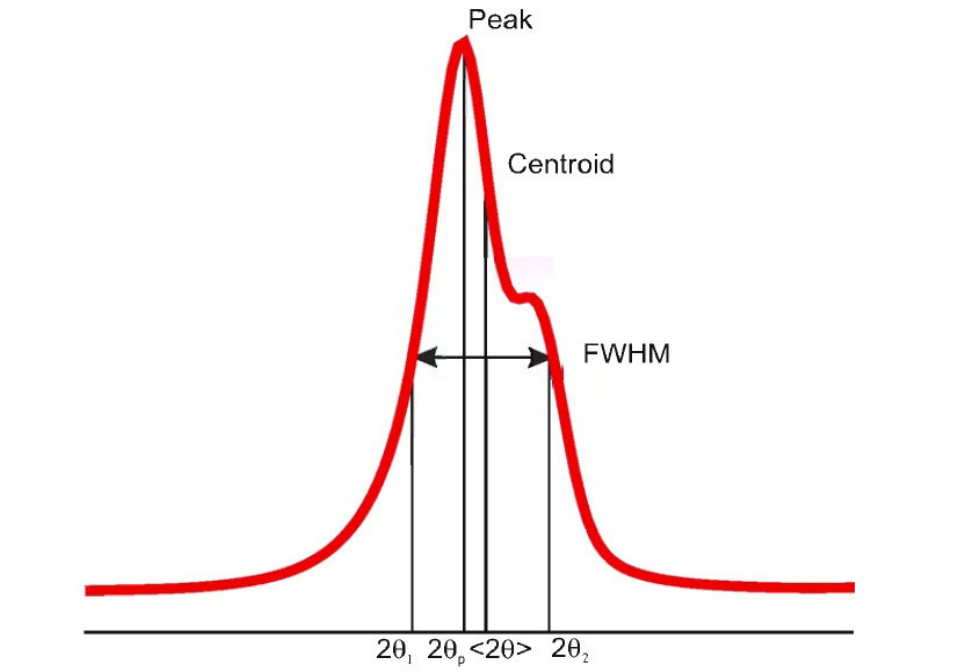

Figure 2: A diffraction line profile illustrating the definition of peak, centroid and full-width at half-maximum intensity (FWHM) [7]

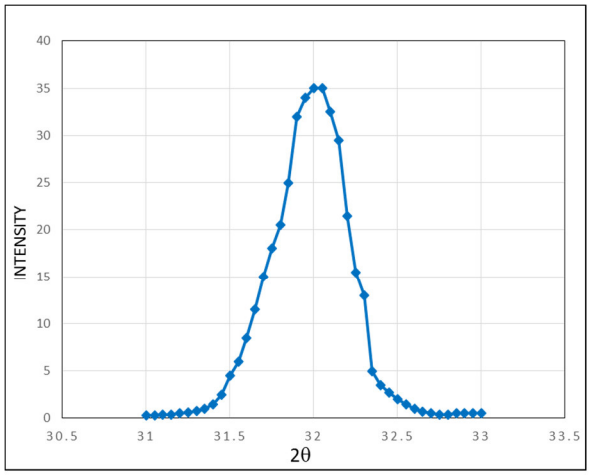

Figure 3: Peak (100) of ZnO nanoparticles for 40 steps

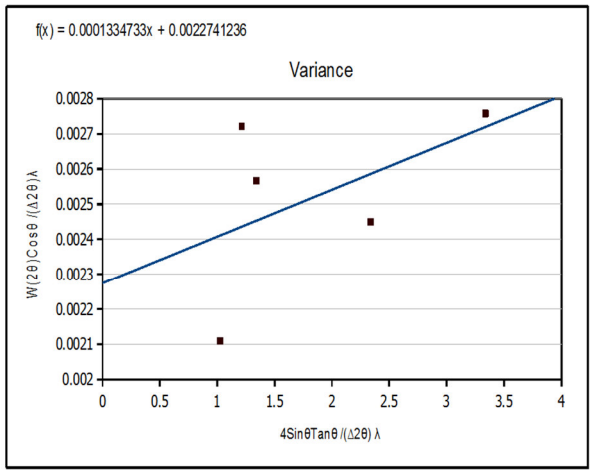

Figure 4: Plot of $W2\theta\ Cos\theta/(\Delta 2\theta)\lambda$ VS $4Sin\theta Tan\theta/\pi\ (\Delta 2\theta)\lambda$ of ZnO nanoparticle

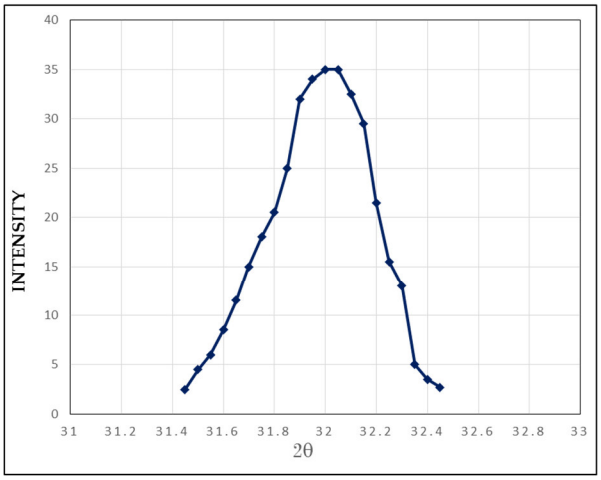

Figure 5: Peak (100) of ZnO nanoparticles for 20steps

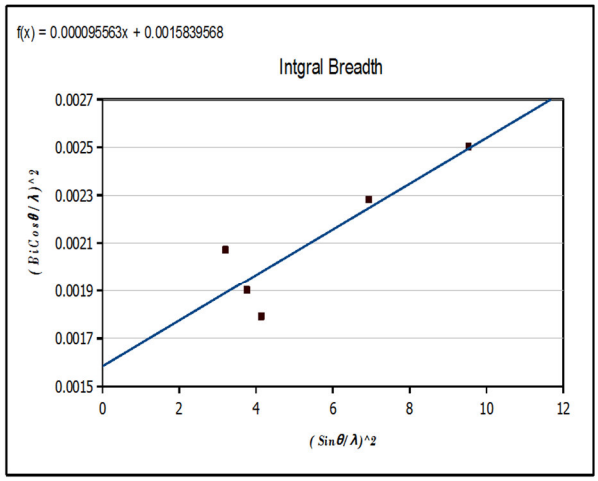

Figure 6: Integral breadth plot of $(\beta_i\ cos\theta)/\lambda)^2$ VS $(sin\theta)/\lambda)^2$ of ZnO nanoparticles

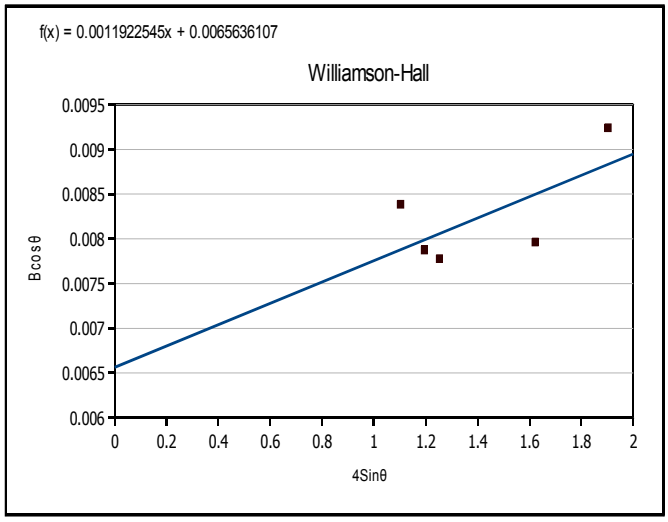

Figure 7 : Williamson-hall plot of $\beta_{hkl}Cos\theta$ VS $4Sin\theta$ of ZnO nanoparticles

Table 1: Variance method for peak (100) of ZnO nanoparticles

No.	2θ	I(2θ)={I-B}	I/I(peak)	2θ. I(2θ)	$(2\theta-\langle 2\theta\rangle)^2$	$(2\theta-\langle 2\theta\rangle)^2$. I(2θ)
1	56	0.8	0.025	1.4	0.715243353	0.017881084
2	56.05	1	0.03125	1.7515625	0.633171292	0.019786603
3	56.1	1.5	0.046875	2.6296875	0.556099231	0.026067151
4	56.15	1.8	0.05625	3.1584375	0.48402717	0.027226528
5	56.2	2	0.0625	3.5125	0.416955108	0.026059694
6	56.25	2.5	0.078125	4.39453125	0.354883047	0.027725238
7	56.3	3.5	0.109375	6.1578125	0.297810986	0.032573077
8	56.35	4.6	0.14375	8.1003125	0.245738925	0.03532497
9	56.4	6	0.1875	10.575	0.198666864	0.037250037
10	56.45	8	0.25	14.1125	0.156594803	0.039148701
11	56.5	11	0.34375	19.421875	0.119522741	0.041085942
12	56.55	14	0.4375	24.740625	0.08745068	0.038259673
13	56.6	21.5	0.671875	38.028125	0.060378619	0.040566885
14	56.65	27	0.84375	47.7984375	0.038306558	0.032321158
15	56.7	29.2	0.9125	51.73875	0.021234497	0.019376478
16	56.75	31	0.96875	54.9765625	0.009162436	0.008876109
17	56.8	32	1	56.8	0.002090374	0.002090374
18	56.85	31	0.96875	55.0734375	1.83132E-05	1.77409E-05
19	56.9	30.5	0.953125	54.2328125	0.002946252	0.002808146
20	56.95	30	0.9375	53.390625	0.010874191	0.010194554
21	57	25	0.78125	44.53125	0.02380213	0.018595414
22	57.05	23	0.71875	41.0046875	0.041730068	0.029993487
23	57.1	20	0.625	35.6875	0.064658007	0.040411255
24	57.15	17.8	0.55625	31.7896875	0.092585946	0.051500933
25	57.2	12	0.375	21.45	0.125513885	0.047067707
26	57.25	6	0.1875	10.734375	0.163441824	0.030645342
27	57.3	4	0.125	7.1625	0.206369763	0.02579622
28	57.35	3	0.09375	5.3765625	0.254297701	0.02384041
29	57.4	2.5	0.078125	4.484375	0.30722564	0.024002003
30	57.45	2	0.0625	3.590625	0.365153579	0.022822099
31	57.5	1.8	0.05625	3.234375	0.428081518	0.024079585
32	57.55	1.5	0.046875	2.69765625	0.496009457	0.023250443
33	57.6	1.1	0.034375	1.98	0.568937396	0.019557223
34	57.65	1	0.03125	1.8015625	0.646865334	0.020214542
35	57.7	1	0.03125	1.803125	0.729793273	0.02280604
36	57.75	1	0.03125	1.8046875	0.817721212	0.025553788
37	57.8	0.8	0.025	1.445	0.910649151	0.022766229
38	57.85	0.5	0.015625	0.90390625	1.00857709	0.015759017
39	57.9	0.3	0.009375	0.5428125	1.111505029	0.01042036
40	57.95	0.05	0.0015625	0.090546875	1.219432967	0.001905364
41	58	0.01	0.0003125	0.018125	1.332360906	0.000416363
			$\sum I/I_{(peak)}$ =12.914375	$\sum 2\theta.I(2\theta)$ =734.1269531		$\sum(2\theta-\langle 2\theta\rangle)^2$ .I(2θ) =0.986043966

Table 2: Calculated the variance of the line profile $W_{2\theta}$ for each peak of ZnO nanoparticles

Peak	$\sum I/I_{(peak)}$	$\sum(2\theta.I(2\theta)$	$<2\theta>$	$\sum(2\theta-<2\theta>)2\ .I(2\theta)$	$W_{2\theta}$
100	11	351.7663	31.97875	0.657048616	0.0597317
002	10.8482	377.2806	34.77818	0.773965278	0.0713451
101	10.81111	394.5528	36.49512	0.742892332	0.0687156
102	12.02	575.2312	47.85617	0.821170649	0.068317
110	12.91438	734.127	56.84572	0.986043966	0.0763524

Table 3: Variance method for each peak of XRD pattern of ZnO nanoparticles

Peak	$W(2\theta)$ corrected	$W(2\theta)_{radian}$	(2θ)	$W(2\theta)Cos\theta\ /\lambda(\Delta 2\theta)$	$4Sin\theta Tan\theta/\lambda(\Delta 2\theta)$
(100)	0.038732	0.000676	32	0.002109018	1.026091031
(002)	0.050345	0.000879	34.75	0.002721712	1.213067162
(101)	0.047716	0.000833	36.5	0.002566958	1.340628558
(102)	0.047317	0.000826	47.85	0.002450015	2.335806952
(110)	0.055352	0.000966	56.8	0.002758108	3.338643746

Table 4: Integral breadth β_i for peak (100) of ZnO nanoparticles

Peak (100)			
No.	**2θ**	**I(2θ)={I-Background}**	**β_i**
1	31.45	2.5	0.0714286
2	31.5	4.5	0.1285714
3	31.55	6	0.1714286
4	31.6	8.5	0.2428571
5	31.65	11.5	0.3285714
6	31.7	15	0.4285714
7	31.75	18	0.5142857
8	31.8	20.5	0.5857143
9	31.85	25	0.7142857
10	31.9	32	0.9142857
11	31.95	34	0.9714286
12	32	35	1
13	32.05	35	1
14	32.1	32.5	0.9285714
15	32.15	29.5	0.8428571
16	32.2	21.5	0.6142857
17	32.25	15.5	0.4428571
18	32.3	13	0.3714286
19	32.35	5	0.1428571
20	32.4	3.5	0.1
21	32.45	2.7	0.0771429
			$(\beta_i)_{Average}$ = **0.504354**

Table 5: β_i and β_{hkl} for each peak of ZnO nanoparticles

Peak	β_i	β_{hkl}	β_{hkl}/β_i
(100)	0.504354	0.5	0.991367
(002)	0.492272	0.4729	0.960648
(101)	0.48413	0.4693	0.969368
(102)	0.540816	0.4993	0.923235
(110)	0.576042	0.602	1.045063

Table 6: Integral breadth method for each peak of XRD pattern of ZnO nanoparticles

Peak	β_i	β_i radian	(2θ)	$(\beta_i cos\theta/\lambda)^2$	$(sin\theta/\lambda)^2$
(100)	0.4180122	0.007296	32	0.0020723	3.201245016
(002)	0.4033521	0.00704	34.75	0.001902	3.757451119
(101)	0.3933706	0.006866	36.5	0.0017913	4.132243372
(102)	0.46135	0.008052	47.85	0.0022826	6.929647743
(110)	0.5021808	0.008765	56.8	0.0025046	9.531706674

Table 7: Calculate FWHM and determine the crystallite size (P) and lattice strain (e) by Scherrer method for each peak of ZnO nanoparticles

Peak	FWHM	FWHM radian	(2θ)	Pnm	$e\ x\ 10^{-3}$
(100)	0.5	0.00872665	32	17.26304736	7.608358
(002)	0.4729	0.00825366	34.75	18.3841131	6.594449
(101)	0.4693	0.00819083	36.5	18.61626321	6.209869
(102)	0.4993	0.00871443	47.85	18.17961628	4.910521
(110)	0.602	0.01050688	56.8	15.66835525	4.858018
				P (average) =17.622 nm	e (average) =6.03624 $x\ 10^{-3}$

Table 8: Williamson-Hall method for each peak of XRD pattern of ZnO nanoparticles

Peak	β_{hkl}	β_{hkl} radian	(2θ)	$\beta_{hkl}Cos\theta$	$4Sin\theta$
(100)	0.5	0.008726646	32	0.0083886	1.102549423
(002)	0.4729	0.008253662	34.75	0.0078771	1.194497592
(101)	0.4693	0.00819083	36.5	0.0077788	1.252655226
(102)	0.4993	0.008714429	47.85	0.0079657	1.622161867
(110)	0.602	0.010506882	56.8	0.0092424	1.902496836

Table 9: The results of variance, integral breadth methods and other methods

Variance method			Integral breadth method		Scherrer method		Williamson-Hall method	
P nm	$< e^2 > x\ 10^{-3}$	$e\ x\ 10^{-3}$	*P nm*	$e\ x\ 10^{-3}$	*P nm*	$e\ x\ 10^{-3}$	*P nm*	$e\ x\ 10^{-3}$
22.276	0.1334733	14.479	25.126	2.443	17.622	6.036	22.063	1.192

Reference

1. Mittemeijerv, E., J. & Welzel, U. (2008), "The "state of the art" of the diffraction analysis of crystallite size and lattice strain", Z.Kristallogr, 223, 552–560.
2. Popović, S. & Skoko, Ž. (2015), "X-Ray Diffraction Broadening Analysis", Macedonian Journal of Chemistry and Chemical Engineering, 34, 1–11
3. Monshi, A., Foroughi, M. R. & Monshi, M. R. (2012), "Modified Scherrer Equation to Estimate More Accurately Nano-Crystallite Size Using XRD", World Journal of Nano Science and Engineering, 2, 154-160.

4. Simm, T. H. (2012). "The use of diffraction peak profile analysis in studying the plastic deformation of metals", Doctor of Philosophy in the Faculty of Engineering and Physical Sciences, A thesis, University of Manchester.
5. Langford, J. I. & Louer, D. (1996), "Powder diffraction", Rep. Prog. Phys., 59, 131–234, Printed in the UK.
6. Langford, J. I. (1968), "The Variance and Other Measures of Line Broadening in Powder Diffractometry. I. Practical Considerations", J. AppL Cryst. , 48, 48-59.
7. Klug, H. P. & Alexander, L. E. (1974), "X-ray Diffraction Procedures for Polycrystalline and Amorphous Materials", New York: Wiley.
8. Sarma, H. & Sarma, K.C. (2014), "X-ray Peak Broadening Analysis of ZnO Nanoparticles Derived by Precipitation method", International Journal of Scientific and Research Publications, 4, 1-7.
9. Sánchez-Bajo, F., Ortiz, A. L. & Cumbrera. F. L. (2006), "Analytical formulation of the variance method of line-broadening analysis for Voigtian X-ray diffraction peaks", J. Appl. Cryst., 39, 598–600.
10. Tripathy, S. N., Mishra, B.G., Shirolkar, M. M., Sen, S., Das, S. R., Janes, D. B. & Pradhan, D. K. (2013), "Structural, microstructural and magneto-electric properties of single-phase $BiFeO_3$ nanoceramics prepared by auto-combustion method", Materials Chemistry and Physics, 1-9.
11. Pradhan D. K. & Tripathy, S. N. (2013), "Effect of Plasticizer Concentration on Microstructural and Dielectric Properties of Polymer Composite Electrolyte", Advances in Chemical Science, 2, 114-121.
12. Khan, A. H. , Bala, P. , Rahman, A. F. M. M. & Nurnabi, M. (2012), "Investigations on Microstructural and Layer Disorder Parameters of Na-Montmorillonite-Glycine Intercalation Compounds", Dhaka Univ. J. Sci., ,60(1), 25-29.
13. Jacob, R. & Isac, J. (2015), "X-ray diffraction line profile analysis of Ba $Sr_{0.6}$ $Fe_{0.4}$ TiO_3 (BSFTO)", International Journal of Chemical Studies, 2(5), pp 12-21
14. Mahalingam, T., John, V. S. & Hsu, L. S. (2007), "Microstructural Analysis of Electrodeposited Zinc Oxide Thin Films", Journal of New Materials for Electrochemical Systems, 10, 9-14.
15. Kim, K., Thanikaikarasan, S., Mahalingam, T., Velumani, S., Kim, T., Kim Y. D. & Asomoza, R. (2009), "Preparation and microstructural studies of electrodeposited FeSe thin films", Advanced Materials Research, 68, 60-68.
16. Ichikawa, R. U., Pereira, L. A. T., Imakuma, K., Turrillas, X. & Martinez, L. G. (2013), "Study on the microstructure of recycled Zircaloy by x-ray diffraction line profile analysis", International Nuclear Atlantic Conference (INAC), Recife, PE, Brazil, 24-29.
17. Venkateswarlu, K., Sreekanth, D., Sandhyarani, M., Muthupandi, V., Bose, A. C. & Rameshbabu, N. (2012), "X-Ray Peak Profile Analysis of Nanostructured Hydroxyapatite and Fluorapatite", International Journal of Bioscience, Biochemistry and Bioinformatics, 2, 389-393.
18. Scardi, P. Leoni, M. & Delhez, R. (2004), "Line broadening analysis using integral breadth methods: a critical review", J. Appl. Cryst. 37, 381–390.
19. Paul, R., Dey, A., Mukherjee, A. K., Sarangi, S. N. &. Pal, A. K. (2012), "effect of nanocrystalline silver impregnation on diamond-like-carbon films by nano-indentation", Indian Journal of Pure & Appliec physics, 50, 252-259.
20. Cerny, R., Joubert, J.M., Latroche, M., Percheron-Guegan, A. & Yvon, K. (2000), "Anisotropic diffraction peak broadening and dislocation substructure in hydrogen-cycled $LaNi_5$ and substitutional derivatives", J. Appl. Cryst., 33, 997-1005.
21. Chowdhury, P.S., Sarkar, A., Mukherjee, P., Gayathri, N., Bhattacharya, M. & Barat, P. (2010), "Studies of microstructural imperfections of powdered Zirconium-based alloys", Materials Characterization, 61, 1061–1065.
22. Prabhu, Y. T., Rao, K. V., Kumar, V. S. S. & Kumari, B. S. (2013), "Synthesis of ZnO Nanoparticles by a Novel Surfactant Assisted Amine Combustion Method", Advances in Nanoparticles, 2, 45-50
23. Serrano, F. J., de Sola, E. R., Kojdecki, M. A., Amigo, J. M. & Alarcon, J. (2008), "Mechanism of Formation of TiO_2-Doped Mullites from Heated Single-Phase Gels Investigated by Structural and Microstructural Parameters", J. American Ceramic Society, 91 [11], 3522–3529
24. Sarkar, A., Bhowmik, A. & Suwas, S. (2009), "Microstructural characterization of ultrafine-grain interstitial-free steel by X-ray diffraction line profile analysis", Appl Phys A, 94, 943–948.
25. George, A., Sharma, S. K., Chawla, S., Malika, M. M. & Qureshi, M.S. (2011), "Detailed of X-ray diffraction and photoluminescence studies of Ce doped ZnO nanocrystals", Journal of Alloys and Compounds, 509, 5942–5946.
26. Zhan, K., Jiang, C. H., Wu, X. Y. & Ji, V. (2012), "Surface Layer Characteristics of S30432 Austenite Stainless Steel after Shot Peening", Materials Transactions, 53, 1002–1006.
27. Shabbir, G., Qureshi, A.H. & Saeed, K. (2006), "Nano-crystalline $LaFeO_3$ powders synthesized by the citrate–gel method", Materials Letters, 60, 3706–3709.
28. Weidenthaler, C. (2011), "Pitfalls in the characterization of nanoporous and nanosized materials", Nanoscale, 3, 792–810.

29. Pang, X., Gao, K., Luo, F., Emirov, Y., Levin, A. A. & Volinsky, A. A. (2009), "Investigation of microstructure and mechanical properties of multi-layer Cr/Cr_2O_3 coatings", Thin Solid Films, 517, 1922–1927
30. Uvarov, V. & Popov, I. (2013), "Metrological characterization of X-ray diffraction methods at different acquisition geometries for determination of crystallite size in nano-scale materials", MATERIALS CHARACTERIZTION, 85, 111 – 123.
31. Kumar, V. S. S. & Rao, K. V. (2013), "X-ray Peak Broadening Analysis and Optical Studies of ZnO Nanoparticles Derived by Surfactant Assisted Combustion Synthesis", Journal Of Nano- And Electronic Physics, 5(2), 02026, 1-6.
32. AL- Jubory, A. A. (2012), "Study on the Effect of Copper Doping on the Structural and Optical Properties of $Cd_{0.7}Zn_{0.3}S$ Nanocrystalline Thin Films Prepared by Chemical Bath DepositionInternational", International Journal of Science and Technology, 2(10), 707-712.
33. Rehani, B. R., Joshi, P. B., Lad, K. N. & Pratap, A. (2006), "Crystallite size estimation of elemental and composite silver nano-powders using XRD principles", Indian Journal of Pure & Applied Physics, 44, 157-161.
34. Prabhu, Y. T., Rao, K. V., Kumar, V. S. S. & Kumari, B. S. (2013), "X-ray Analysis of Fe doped ZnO Nanoparticles by Williamson-Hall and Size-Strain Plot", International Journal of Engineering and Advanced Technology (IJEAT), 2, 268-274.
35. Prabhu, Y. T. Rao, K. V. Kumar, V. S. S. & Kumari, B. S. (2014), "X-Ray Analysis by Williamson-Hall and Size-Strain Plot Methods of ZnO Nanoparticles with Fuel Variation", World Journal of Nano Science and Engineering, 4, 21-28.
36. Kumar, L., Kumar, P., Narayan, A. & Kar, M. (2013), "Rietveld analysis of XRD patterns of different sizes of nanocrystalline cobalt ferrite", International Nano Letters, 3(8), 1-12
37. Mitra P. & Mondal, S. (2013), "Structural and Morphological Characterization of ZnO thin films Synthesized by SILAR", Progress in Theoretical and Applied Physics, 1, 17-31.